Hindawi
Journal of Advanced Transportation
Volume 2024, Article ID 3414116, 15 pages
https://doi.org/10.1155/2024/3414116

Research Article

Impact of Driver Compliance and Aggressiveness in Connected Vehicles on Mixed Traffic Flow Efficiency: A Simulation Study

Chenhao Qian,[1] **Taojun Feng**,[2] **Zhiyuan Li**,[2] **Yanjun Ye**,[1] **and Shengwen Yang**[1]

[1]*College of Machinery and Transportation, Southwest Forestry University, Kunming 650000, China*
[2]*Power China Sichuan Electric Power Engineering Co., Ltd., Chengdu 610016, China*

Correspondence should be addressed to Shengwen Yang; yangshengwen@swfu.edu.cn

Received 10 October 2023; Revised 20 November 2023; Accepted 1 April 2024; Published 2 May 2024

Academic Editor: Juneyoung Park

Connected vehicles (CVs) are becoming increasingly prevalent in today's transportation systems, and understanding their behavior in mixed traffic flow is crucial for enhancing traffic efficiency and safety. This paper presents a comprehensive study investigating the impact of CV drivers' compliance and aggressiveness on mixed traffic flow through simulation experiments. The unique contribution of this research lies in the adoption of a clustering method to classify CV drivers' compliance and aggressiveness based on trajectory data captured by Unmanned Aerial Vehicles (UAVs). This approach allows for the accurate calibration of car-following and lane-changing models, surpassing previous methodologies. The study outlines two primary methods: the intelligent driver model (IDM) with driver compliance (CVs-IDM) and the lane-change 2013 model with drivers' style. These methods are applied to simulate various scenarios of mixed traffic flow, considering different CV penetration rates and driver types. The pivotal findings reveal that higher CV penetration rates lead to reduced traffic flow disturbance, improved safety, and enhanced efficiency. Specifically, CV drivers exhibiting high compliance and normal aggressiveness demonstrate optimal performance in terms of disturbance reduction, safety, and overall efficiency. This research offers valuable insights for policymakers and practitioners. It recommends increasing the CV penetration rate in mixed traffic flow to enhance overall efficiency. Moreover, selecting the appropriate CV driver type based on the penetration rate can further optimize traffic flow, positively impacting transportation systems and promoting safer and more efficient mixed traffic environments.

1. Introduction

With the advances in Information and Communication Technologies (ICT), it allows the transportation community which includes vehicle-to-vehicle and vehicle-to-infrastructure or vehicle-to-everything communications to foresee dramatic improvements in the next few years in terms of a more efficient, environmentally friendly, and safe traffic management. Guériau et al. [1] believed that the connected vehicles could exchange information with infrastructure and realized vehicle-to-vehicle communication. Previous studies generally believed the connected vehicles (CVs) could improve the safety and efficiency and decrease the disturbance in traffic flow and decrease emission [2–6].

The current studies on mixed traffic flow are mainly divided into the following categories: automated vehicles (AVs) and traditional vehicles (TVs) [7–10], connected and automated vehicles (CAVs) and TVs [11–14], adaptive cruise control (ACC) and TVs [15], and CVs and TVs [16–24]; Saifuzzaman and Zheng, 2014; [12, 25–28]. The mixed traffic flow mentioned later in this study represents the mixed traffic flow of CVs and TVs.

The research of Rahman et al. [18] showed that networked and connected and autonomous vehicles (CAVs) can be connected to each other. Therefore, CV is expected to reduce human driver errors and improve traffic efficiency and safety. The use of connected vehicles (CVs) can significantly increase the expected capacity, which will also enable more efficient use of the existing transportation

infrastructure, resulting in reduced traffic congestion and time loss, which in turn improves the quality of traffic flow [19, 20, 22–24]. The research of Van Arem et al. [21] showed that CV mixed traffic will be able to promote more efficient traffic and the penetration of CV vehicles will also reduce congestion [29–32]. Ni et al. [32] modified the reaction time parameters of the car-following model to distinguish CVs and TVs by numerical simulation of mixed traffic flow and showed that higher CV proportion leads to higher lane capacity. Zheng et al. [5] introduced the prospect theory based on IDM (a car-following model) to model the CVs drivers' compliance to continuous information. This study divided CVs drivers' compliance into two types: high compliance and low compliance, and got the way to calibrate the parameters in car-following model based on two types of compliance. Based on previous study on drivers' compliance, Zheng et al. [4] analyzed the impact of CV proportion and spatial arrangement of mixed traffic flow on mixed traffic flow disturbance, efficiency, and safety and showed that the best spatial arrangement for mixed traffic flow and higher CV proportion lead to smaller disturbance, higher efficiency, and higher safety.

However, few studies considered the combination between car-following and lane-changing behaviors and degree of desire for lane-changing of CVs. And present studies lack effective methods to calibrate the parameters in the car-following and lane-changing models. Besides, most of the simulation scenes set in previous studies are too simple to get more specific, systematic conclusions. But in real condition, the conclusion drawn by simulation experiments should be used in complex scene, such as multilane and multiway sections. Last but not least, very few previous studies established suitable evaluation models to qualify the overall efficiency of mixed traffic flow in each case designed in experiment.

Motivated by the limitations and gaps mentioned above, this study used a multivariate clustering method to classify the different degrees of compliance and aggressiveness of CV drivers and further calibrate the parameters of the three compliance levels of the car-following model (CVs-IDM (high compliance), CVs-IDM (average compliance), and CVs-IDM (low compliance)) and lane-changing model (aggressive-LC2013, average aggressive-LC2013, and normal-LC2013). Based on calibration results, we set up mixed traffic flow for the simulation experiment. Then, we designed two simulation experiments to investigate the impact of lane-changing traffic on traffic flow disturbance, safety, and efficiency of mixed traffic flow on three tested lanes. Moreover, we set up eight cases for the simulation experiment according to the different behaviors of CV drivers and the different spatial arrangement of mixed traffic flow. Then, we established the collaborative evaluation model to calculate the values of overall efficiency corresponding to eight cases and selected the case which has highest value of overall efficiency when the CV proportion is 80% and 20%, respectively. At last, we deduced the car-following and lane-changing models that CV drivers should obey under different CV proportions in mixed traffic flow, through further experiments.

2. Methodology

2.1. Car-Following Model with Driver Compliance. The intelligent driver model (IDM) is employed to model car-following behavior of TVs which is widely used in various traffic simulation software programs. IDM belongs to the category of desired measures models and assumes that the acceleration is a continuous function of driver's spacing and speed to the leader (which is represented in equation (1)), and speed difference between the leader and the follower (which is represented in equation (2)).

$$a_n\left(S_n, V_n, \Delta V_n\right) = a\left[1 - \left(\frac{aV_n}{V_0}\right)^{\delta} - \left(\frac{S^*\left(V_n, \Delta V_n\right)}{S_n}\right)^2\right], \tag{1}$$

$$S^*\left(V_n, \Delta V_n\right) = \mathrm{s}_0 + \max\left(0, TV_n + \frac{V_n \Delta V_n}{2\sqrt{ab}}\right), \tag{2}$$

where the parameters δ, V_0, T, s_0, a, and b represent free acceleration exponent, desired speed of vehicles, desired time interval, standstill distance, maximum acceleration, and desired deceleration of vehicle, respectively. Besides, a_n represents the IDM acceleration, s^* represents the desired spacing, V_n represents the speed, ΔV_n represents the relative speed between leader's speed and follower's speed, and S_n represents the space interval between leader and follower.

However, different drivers have different degrees of compliance to continuous information. And the continuous information includes space interval and relative speed between two vehicles and is delivered from the leader to the next follower, which has a significant effect on reducing traffic accidents. Based on the above difference, we further establish IDM with driver compliance (CVs-IDM) which is applied in CVs in this study. The CVs-IDM is presented as follows:

$$a_n(S_n, V_n, \Delta V_n) = a\left[1 - \left(\frac{aV_n}{V_0}\right)^{\delta} - \left(\frac{S^*(V_n, \Delta V_n)}{S_n}\right)^2\right], \tag{3}$$

$$S^*(V_n, \Delta V_n) = s_0 + (1 + \mathrm{UT}(h_{obs}))TV_n + \frac{V_n \Delta V_n}{2\sqrt{ab}}. \tag{4}$$

Different from IDM, we multiply $(1 + \mathrm{UT}(h_{obs}))$ and time interval parameters TV_n to measure the degree of driver's compliance. Refer to Sharma et al. [33]; $\mathrm{UT}(h_{obs})$ is the utility value calculated at h_{obs} using prospect theory shape parameters α, γ, and λ. h_{obs} is the observed headway between the follower and the leader measured at the time when the messages are received by the followers. So, we divide high compliance (HC), low compliance (LC), and average compliance (AC) by setting parameter α, γ, and λ values according to Sharma et al. [33]. Figure 1 shows the usefulness curves for high\average\low compliance drivers, which are developed by formulation:

$$V(h_{\mathrm{obs}}) = \frac{1}{\left(1 + e^{\lambda(\mathrm{ah_{obs}}\text{-}1)}\right)} \tag{5}$$

This formulation shows that the usefulness of continuous information to drivers depends on h_{obs}. Besides, we can learn from Figure 1 that high compliance driver has a higher usefulness value than low compliance driver with the same observed headway.

2.2. Lane-Changing Model with Drivers' Style

2.2.1. LC2013 Model. In this study, we choose LC2013 model as the basic lane-changing model which is suitable for multilane autonomous driving simulation. Similar to IDM, we apply this calibrated lane-changing model to TVs. Different from other micro-lane-changing models, the LC2013 model clearly distinguishes four different lane-changing motives: strategic change, cooperative change, tactical change, and obligatory change.

(1) *Strategic Change*. Strategic change mainly includes two steps: evaluating subsequent lanes and determining urgency lane. First, there are two types of lane information that can be evaluated, i.e., for every lane on the current edge, a sequence of lanes that can be followed without lane changing up to the next dead end or to a maximum distance and for every lane on the current edge, the traffic density along the best lanes and for every lane on the current edge, the offset in the lane index to the lane which is strategically advisable. Besides, the method to determine urgency is shown in equation (6); if this equation holds true, we can determine this urgency lane.

$$d - o < \mathrm{lookAheadSpeed} \times |\mathrm{BestLane}Offset| \times f, \tag{6}$$

where d represents the distance between vehicle and the end of dead lane; o is determined by lane occupation; and f is the time required to change lane.

(2) *Cooperative Change*. In some practical situations, the main purpose of a vehicle performing lane-changing is to help another vehicle change lanes. In the LC2013 model, the vehicle is notified by other vehicles that it is blocking the following vehicle. If there is no strategic reason against changing lanes, the vehicle can change in any possible direction to create space interval for blocked vehicles.

(3) *Tactical Change*. Tactical lane change is when the vehicle tries to avoid following the slow leader and performing lane-changing, the purpose of which is to increase the own speed. In the LC2013 model, parameter speedGainProbability is produced to measure the likelihood of a vehicle changing lane to increase speed. This parameter is incrementally updated in each simulation step and reset when changing lane to prevent oscillation. This parameter is calculated by equations (7) and (8):

$$\mathrm{speedGain\ Probability} \coloneqq \mathrm{speedGain\ Probability} + \frac{(v - u)}{v}, \tag{7}$$

$$\mathrm{speedGain\ Probability} \coloneqq \mathrm{speedGain\ Probability} - \frac{(v - u)}{v}, \tag{8}$$

where v represents the desired speed in right lane and u represents the desired speed in left lane. If the desired speed in left lane is faster than that in right lane, we use equation (7) to update the parameter. On the contrary, if the desired speed in left lane is slower, we use equation (8) to update the parameter.

(4) *Obligatory Change*. Obligatory change can also be called Obligation to clear the overtaking lane, which refers to avoiding forced lane changes and helping other faster vehicles in lane. In the LC2012 model, parameter keepRightProbability is produced to measure the likelihood of keeping the vehicle on the

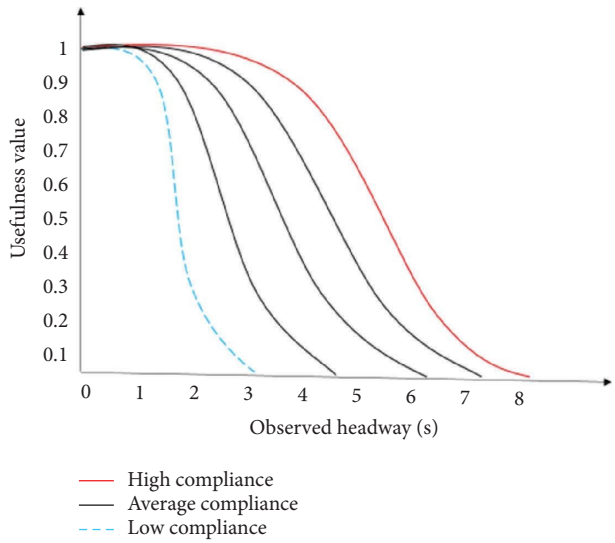

Figure 1: Difference between usefulness value function curves of high compliance, average compliance, and low compliance levels.

right lane, which is updated in each simulation step. This parameter is calculated by the following equation:

$$\text{keepRight Probability} := \text{keepRight Probability} - \frac{(t \times L)}{(V \times v \times T)}, \tag{9}$$

where L represents the max speed permitted in lane; V is the max desired speed in lane; v represents the current speed; and T is calibration parameter which is set to 5 in this study.

2.2.2. LC2013 Model with Drivers' Style. During the total lane-changing process, the performance of drivers can be divided into two parts: aggressive and normal. And the difference between drivers' lane-changing style is a significant factor affecting the driving safety of vehicle. So, we introduce the drivers' style to CVs' lane-changing model (CVs-LC2013) to simulate the traffic process of CVs. Aggressive-LC2013 model and normal-LC2013 model are, respectively, applied in above two kinds of CVs, in this study. According to the demands of the control group in the experiment, we further establish the average aggressive-LC2013 model.

2.3. Calibration of CVs' Car-Following and Lane-Changing Models

2.3.1. Study Scene. In this study, a 210-meter section located on Qujiang interchange in Wuhan, Hubei, was used (Figure 2). The study scene was divided into two parts: a 70-meter traffic flow input section and a 140-meter traffic flow test section. Traffic flow input consists of one General Purpose Lane (GPL) and two Managed Lanes (MLs). Traffic flow test section consists of two General Purpose Lanes (GPLs) and two Managed Lanes (MLs).

2.3.2. Parameter Calibration Based on Trajectory Indicator Clustering. This study got the indicators values which is related to drivers' compliance when performing car following (in Table 1) and aggressiveness when performing lane changing (in Table 2) by using of the UAV's capture of CVs trajectory data in the study scene. Tables 1 and 2, respectively, list the indicators connected to CVs drivers' compliance and aggressiveness. Then, we clustered the above indicator values in the trajectory data, respectively (set the number of clusters to 3), to distinguish the high compliance (HC), low compliance (LC), and average compliance (AC) and aggressive, normal, and average aggressive behaviors of drivers. Furthermore, we can control and reflect the driver's style (compliance and aggressiveness) by setting the size of the parameters in Tables 1 and 2. For example, higher compliance of drivers corresponds to lower $\Delta v'$ (the difference between the minimum and maximum speed of CV during the driving on the section).

The smaller the indicators values in Tables 3 and 4, the higher the degree of compliance and aggressiveness of the CV drivers. Moreover, the values of component 1 are 93.03% and 98.89%, respectively, in Figures 3(a) and 3(b). So, the smaller the value of the cluster center on the component axis, the higher the compliance and aggressiveness. In Figure 3(a), cluster 1, cluster 2, and cluster 3 correspond to high

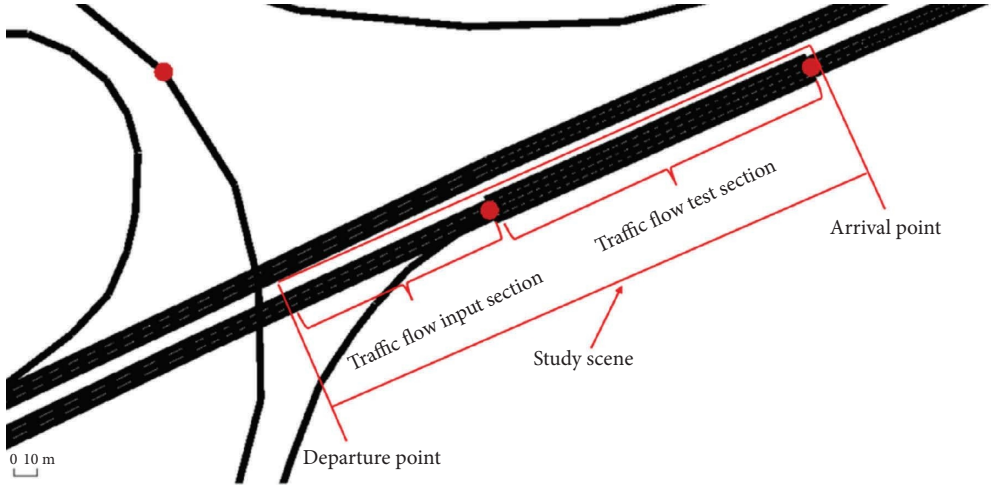

Figure 2: Study scene in this study.

Table 1: Indicators related to driver compliance when perform car-following.

Indicators	Definition
$\Delta v'$	The difference between the minimum and maximum speed of CV during driving on the section
$\Delta a'$	The difference between the minimum and maximum acceleration of CV during driving on test section
$\Delta x'$	The difference between the minimum and maximum gap of CV during driving on test section

Table 2: Indicators related to driver aggressiveness when perform lane-changing.

Indicators	Definition
LCD	The total time required for CV to travel from the current lane to the target lane
DT	The distance from the center line of the CV to the right most edge of the lane, up to the moment the CV changes lane
$\Delta v''$	The speed difference between the CV and the vehicle ahead
$\Delta x''$	The distance between the CV and the vehicle ahead when the lane change is just completed

compliance, average compliance, and low compliance, respectively. In Figure 3(b), cluster 1, cluster 2, and cluster 3 correspond to average aggressive, aggressive, and normal, respectively. Furthermore, based on the results of the CV driver behavior clustering, we use the basic parameter values of the CVs' lane-changing models and car-following models in each cluster to calibrate the basic parameters of the CVs' lane-changing models and car-following models set in the simulation experiment in this study. The calibration results are shown in Tables 2 and 4.

K_s represents the desire to perform strategic change; K_c represents the desire to perform cooperative change; K_k represents the compliance with the right-hand driving rule which is connected with tactical change; K_{sub} represents the desire to use the horizontal arrangement in the lane; K_p represents the desire to invade other lane which is connected to obligatory change.

3. Indicators of Traffic Flow Disturbance, Safety, and Efficiency

3.1. Traffic Flow Disturbance. We analyze traffic flow disturbance in terms of traffic oscillation measures such as oscillation duration and oscillation amplitude (the bigger parameters correspond to bigger traffic flow disturbance). This study calculates oscillation duration and oscillation amplitude specifically by adopting wavelet energy. According to the speed curve of the vehicle in simulation period, the corresponding energy curve can be generated at the same time. The moment vehicle is accelerating or decelerating, there appears a peak or valley in energy curve to calculate oscillation duration and oscillation amplitude. The relationship of speed curve and energy curve is shown in Figure 4. The wavelet energy can be expressed as

Table 3: Calibrated parameters in CV's car-following models applied in study (CVs-IDM (LC), CVs-IDM (HC), and CVs-IDM (AC)).

Parameters	CVs					
	CVs-IDM (LC)		CVs-IDM (HC)		CVs-IDM (AC)	
	Calibrate	P value	Calibrate	P value	Calibrate	P value
V_0 (m/s)	26.5	0.045	26.5	0.009	26.5	0.034
δ	4	0.037	4	0.035	4	0.039
s_0 (m)	4.5	0.0008	4.5	0.044	4.5	0.046
T (s)	1.2	0.003	1.2	0.042	1.2	0.042
a (m/s^2)	3	0.042	3	0.008	3	0.003
b (m/s^2)	3	0.037	3	0.027	3	0.006
α	0.6	0.008	0.25	0.035	0.44	0.031
γ	0.7	0.0064	0.7	0.044	0.7	0.021
λ	6.5	0.033	9.5	0.003	7.7	0.024

Table 4: Calibrated parameters set in lane-changing models in study (LC2013, normal-LC2013, aggressive-LC2013, and average aggressive-LC2013).

Parameters	CVs					
	Normal-LC2013		Aggressive-LC2013		Average aggressive-LC2013	
	Calibrate	P value	Calibrate	P value	Calibrate	P value
K_s	1	0.03	100	0.032	65	0.002
K_c	1	0.032	0.5	0.04	0.74	0.003
K_k	1	0.022	1	0.029	1	0.033
K_{sub}	1	0.027	100	0.045	55	0.044
K_p	0	0.007	0.2	0.008	0.12	0.022
Assertive	1	0.038	1.5	0.006	1.3	0.007
AvgaccelLat	4.55	0.047	5	0.012	4.76	0.008
MaxaccelLat	52.43	0.007	113.16	0.017	78.92	0.031
LookaheadLeft	2	0.006	2	0.04	2	0.033
MaxSpeedLatFactor	1	0.035	1	0.003	1	0.028
AvgSpeedLat	0.71	0.009	0.54	0.006	0.66	0.022
MaxSpeedLat	5.25	0.005	10.28	0.011	7.89	0.004

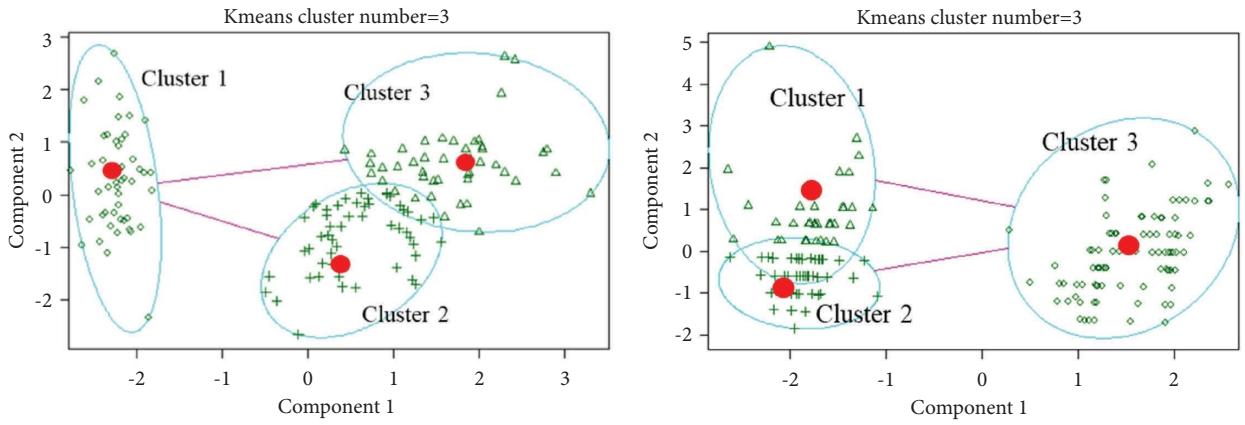

Figure 3: Indicators of multivariate clustering. (a) Indicators connected to drivers' compliance. (b) Indicators connected to drivers' aggressiveness.

$$E_n = \frac{1}{\max(m)} \int_0^{\infty} |T(m,n)^2|. \tag{10}$$

The wavelet coefficient $T(m,n)$ can be calculated as

$$T(m,n) = \frac{1}{\sqrt{a}} \int_{-\infty}^{+\infty} S(t)\psi \frac{t-m}{n} \mathrm{d}t, \tag{11}$$

where S_t represents the time series of speeds; $\int_{-\infty}^{+\infty} S(t)\psi t - m/n$ is the function describing wavelet; and m and n are upper bound and lower bound of time range in wavelet function.

Based on the wavelet energy of vehicle, we can further calculate oscillation duration, oscillation amplitude, average oscillation duration, and average oscillation amplitude, respectively.

$$\text{Oscillationduration} = t_i - t_j, \tag{12}$$

$$\text{Averageoscillationduration} = \sum_{p=1}^{p=k} \frac{OD_p}{k}, \tag{13}$$

$$\text{oscillationamplitude} = |v_{t_j} - v_{t_i}|, \tag{14}$$

$$\text{Averageoscillationamplitude} = \sum_{p=1}^{p=k} \frac{OA_p}{k}, \tag{15}$$

where t_i and t_j represent the appearing time of first peak and second peak, respectively; OD_p represents the oscillation duration of p^{th} vehicle; v_{t_i} and v_{t_j} represent the speed of t_i and t_j; and OA_p represents the oscillation amplitude of p^{th} vehicle.

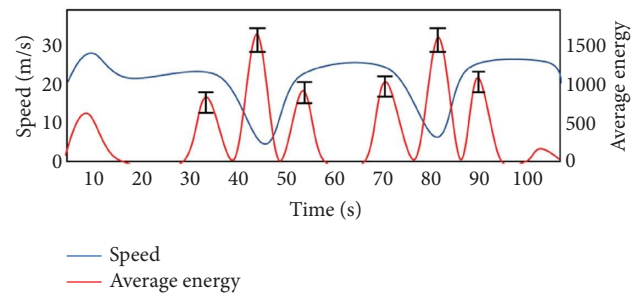

Figure 4: Illustrations of traffic oscillation and corresponding detection using wavelet-based energy.

3.2. Traffic Flow Safety. This study uses TGAP (the bigger value corresponds to higher safety) and DRAC (the bigger value corresponds to less safety) to represent the degree of traffic safety. Among them, the TGAP is vehicle's time headway to the leading one which can be calculated in equation (16). And DRAC is deceleration rate to avoid the crash which can be calculated in equation (17). Besides, higher TGAP and lower DRAC means higher safety, and we set up maximumTGAP and minimumDRAC to measure the safety of traffic flow on a lane which are calculated in equations (18) and (19). Furthermore, we use average TGAP and average DRAC to measure the safety of whole traffic flow on all lanes which are calculated in equations (20) and (21):

$$\text{TGAP} = \frac{S_n}{v}, \tag{16}$$

$$\text{DRAC} = \frac{(\Delta V_n)^2}{S_n}, \tag{17}$$

$$\text{maximumTGAP} = \max(\text{TGAP}_1, \text{TGAP}_2, \text{TGAP}_3, \ldots\ldots, \text{TGAP}_r), \tag{18}$$

$$\text{minimumDRAC} = \min(\text{DRAC}_1, \text{DRAC}_2, \text{DRAC}_3, \ldots\ldots, \text{DRAC}_r), \tag{19}$$

$$\text{AverageTGAP} = \frac{\sum_{l=1}^{q} \text{TGAP}_l}{q}, \tag{20}$$

$$\text{AverageDRAC} = \frac{\sum_{l=1}^{q} \text{DRAC}_l}{q}, \tag{21}$$

where S_n represents the space gap between leader vehicle and follower vehicle; v represents the speed of follower vehicle; ΔV_n represents the relative speed of leader vehicle and follower vehicle; r represents the amount of vehicle contained in traffic flow on one lane; and q represents the amount of vehicle contained in all traffic flows on the whole lanes.

3.3. Traffic Flow Efficiency. This study uses x-t method to calculate flow (q) and speed (V) of traffic flow based on Edie's generalised definition (Edie, 1963). Because the trajectory data of each vehicle are known in this study which are needed by Edie's generalised definition, we can further generate x-t diagram of all vehicles as shown in Figure 5. By

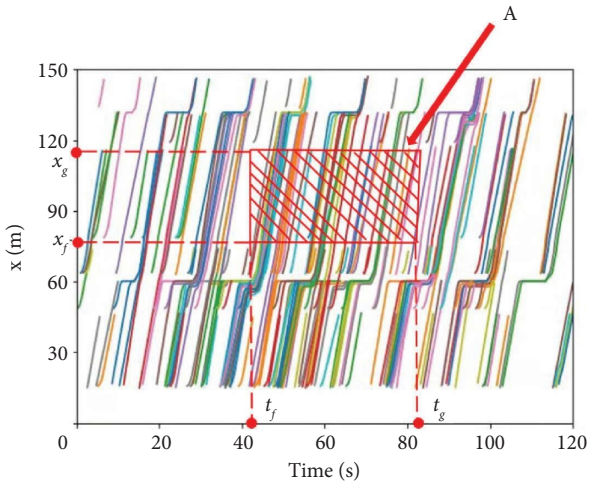

FIGURE 5: x-t diagram of all vehicles in simulation scene which can be used to calculate flow and speed according to Edie's generalised definition.

this way, we can calculate the flow and speed using x-t method as shown in equations (22) and (23):

$$q = \frac{d(A)}{|A|}, \tag{22}$$

$$V = \frac{d(A)}{t(A)}, \tag{23}$$

where $d(A)$ represents total distance of all vehicles in A; $t(A)$ represents total time of all vehicles in A; and $|A|$ represents the area of A which can be calculated as follows:

$$|A| = \left(x_g - x_f\right) \times \left(t_g - t_f\right). \tag{24}$$

4. Mixed Traffic Flow Experiments

4.1. Environmental Description. In the experimental setup of this paper, the simulation environment follows general road design standards.

(1) *Traffic Flow Input Phase*

Basic Flow. Three basic flows represent different types of vehicle flows, with an average lane width of 3.75 meters for each flow.

Lane-Change Flow. The lane-changing flow merges into lanes with standard lane width of 3.75 meters.

(2) *Traffic Flow Test Phase*

Lane Structure. The traffic flow test phase comprises four lanes, each with a standard lane width of 3.75 meters.

Relative Lane Positions. After the intersection, the distance from the center line of one lane to the center line of the adjacent lane is the standard lane width, ensuring sufficient space for normal driving and lane-changing operations.

Geometric Features of the Intersection. The length of the lane merging area at the intersection is twice the standard lane length, i.e., 7.5 meters. Additionally, geometric features such as curvature and entry angle at the intersection adhere to general urban road design standards.

(3) *Lateral Gap between Lanes*. A lateral gap of half the standard lane width of 1.87 meters is maintained between lanes to ensure an adequate safety distance between vehicles.

The initial layout of vehicles is achieved by considering the initial positions and quantities of different vehicle types. Special attention is given to the mixed traffic flow of basic flows 1, 2, and lane-changing flow, as well as the TV flow in basic flow 3. The composition of vehicles in the lane-changing flow is explicitly defined, including four CVs changing from lane 1 to lane 2, and four TVs changing from lane 3 to lane 4. CVs in the lane-changing flow are modeled using CVs-IDM (AC) and average aggressive-LC2013. Randomness in traffic flow is considered at the microscopic level of vehicle behavior, such as the stochastic variation of acceleration, and is integrated into the model through probabilistic modeling of vehicle behavior.

4.2. Statistical Assumptions. A car's speed is primarily determined by the vehicles in front of it or in the target lane. A vehicle may only execute a lane change when there is sufficient physical space in the target lane, ensuring that it does not get too close to the vehicles in front and behind in the target lane. In each simulation step, vehicles execute the following substeps sequentially:

(1) Compute priority alternative lanes.

(2) Calculate the assumed safe speed for staying in the current lane, considering the speed requirements related to lane change from the previous simulation step.

(3) Lane change model computes the need for a lane change.

(4) Either execute the lane change or calculate the required speed for the next simulation step. The decision to change speed depends on the urgency of the lane change request.

The model in this paper explicitly distinguishes four different lane-change motivations: strategic change, cooperative change, tactical change, and obligatory change.

4.2.1. Strategic Change. Strategic lane changes occur when there is no direct connection between the current lane of a vehicle and its intended target lane. For vehicles intending to proceed straight, a left-turn lane creates a terminating path, prompting vehicles to strategically change lanes in advance, provided there are no obstructive factors. Due to the critical importance of strategic lane changes in overall traffic planning, we establish a cautious adjustment strategy

for the ego vehicle to ensure the successful implementation of lane changes.

4.2.2. Cooperative Change. In certain scenarios, vehicles change lanes to assist other vehicles in smoothly entering the current lane. In the current model, vehicles are identified by other vehicles as potential hindrances to the following vehicle. Unless there are explicit strategic reasons preventing a lane change, the ego vehicle can change lanes in any direction to create space for obstructed vehicles. Vehicles unable to engage in cooperative lane changes can slightly adjust their speed to increase the probability of successful lane changes in subsequent simulation steps.

4.2.3. Tactical Change. Tactical lane changes involve balancing the expected speed gain with the effort required for the lane change. The speedGainProbability is utilized to measure the likelihood of a vehicle changing lanes to increase speed. This probability is incrementally adjusted in each simulation step and reset during a lane change to prevent oscillations.

4.2.4. Obligatory Change. The compulsory action of clearing the overtaking lane is considered a collaborative behavior as it aids fast-moving vehicles. This behavior is mandated by traffic regulations. In the current lane-change model, each vehicle maintains a variable, keepRightProbability, which decreases over time. Once it falls below a threshold of −2, it triggers a right lane change (using negative values to represent the variability of speedGainProbability). The keepRightProbability p: is updated as follows:

$$p \coloneqq p - \frac{t * L}{V * v * T}, \tag{25}$$

where L is the legal speed limit on the current road, V is the ego vehicle's maximum expected speed, V is its current speed, and T is a calibration parameter currently set to 5.

4.3. Mixed Traffic Flow in Simulation Experiment. Figure 6 displays the direction of each traffic flow on MLs and GPLs in simulation experiment.

Basic flow 1, basic flow 2, and lane-change flow are mixed traffic flow and basic flow 3 is TV flow. The composition of lane-change traffic flow is certain, in which four CVs change lane to lane 1; four CVs change lane to lane 2; four TVs change lane to lane 3 and four TVs change lane to lane 4, respectively. And CVs contained in lane-change traffic flow are subject to CVs-IDM (AC) and average aggressive-LC2013. Meanwhile, when we use UAV to capture the trajectory data of vehicles on the traffic flow test section, we find that the traffic efficiency and speed of lane 4 are far lower than the other three lanes, which has little reference significance for researching safety and other indicators. Therefore, we only analyze specific indicators for lanes 1, 2, and 3. Then, we set up two spatial arrangement methods for the three basic traffic flows on traffic flow input section. In the first case of traffic flow spatial arrangement, the penetration rate of CV on MLs is 80%. In the second case of mixed traffic flow spatial arrangement, the penetration rate of CV on MLs is 20%. Moreover, considering the arrangement of CVs and TVs on the traffic flow input section contained in each group mixed traffic flow will have a great impact on the experiments results; therefore, this study sets the arrangement of CVs and TVs on MLs to be arranged by the best arrangement (shown in Figure 7) [4]. When the arranged traffic flow enters the traffic flow test section, the arrangement of CVs and TVs on each lane will be changed due to the influence of the lane-change traffic flow. Table lists the specific experiments designed in this study.

4.4. Experiment Design. We set up three experiments for three measured indicators (mixed traffic flow disturbance, safety, and efficiency). According to the difference between CV penetration rate in the mixed traffic flow, the lane-change model, and the car-following model of CV, we set up eight cases for each experiment. Table 5 lists the specific experiments designed in this study.

4.5. Experiment Results

4.5.1. Experiment 1 (Mixed Traffic Flow Disturbance). The purpose of this experiment is to investigate the difference of traffic flow disturbance of eight cases on entire traffic flow test section. We number the CVs on lane 1, lane 2, and lane 3 as 1 to 10, 11 to 20, and 21 to 30, respectively. Figure 8 displays the simulation experiment results.

In case of CV penetration rate being 80%, the traffic flow disturbance of HC-normal-CV is far less than other three kinds of CV although the difference in indicator duration is not so obvious. In general, normal-CV leads to less traffic flow arrangement than aggressive-CV by comparing HC-aggressive-CV and HC-normal-CV and LC-aggressive-CV and LC-normal-CV, respectively. And HC-CV leads to less traffic flow disturbance than LC-CV by comparing HC-aggressive-CV and LC-aggressive-CV and HC-normal-CV and LC-normal-CV, respectively. And we can get the same conclusion in case of CV penetration rate being 20%.

Moreover, from lane 1 to lane 3, the gap between the eight cases gradually decreases. And compared with the mixed traffic flow with lower CV penetration rate, the mixed traffic flow with higher CV penetration rate corresponds to lower traffic flow disturbance.

4.5.2. Experiment 2 (Mixed Traffic Flow Safety). The purpose of this experiment is to investigate the difference of traffic flow safety of eight cases on entire traffic flow test section. Figure 9 displays the simulation experiment results.

In case of CV penetration rate being 80%, the traffic flow safety of HC-normal-CV is far higher than other three kinds of CV. In general, normal-CV leads to higher traffic flow safety than aggressive-CV by comparing HC-aggressive-CV and HC-normal-CV and LC-aggressive-CV and LC-normal-CV, respectively. And HC-CVs lead to higher traffic flow safety than LC-CV by comparing HC-aggressive-CV

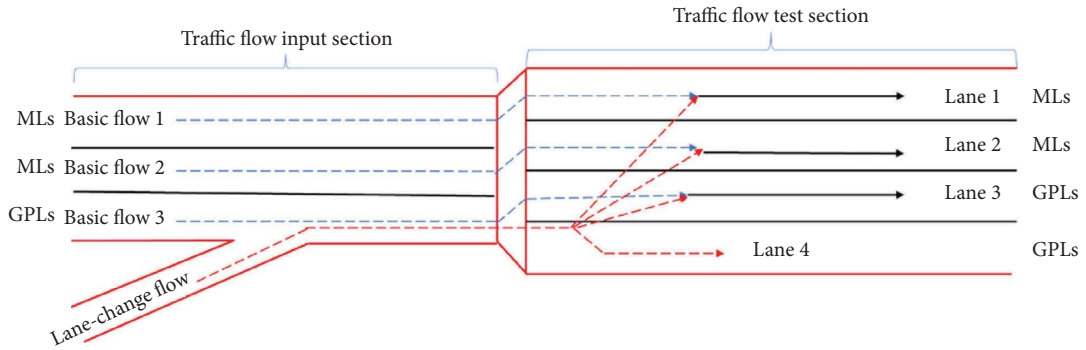

Figure 6: Direction of each group mixed traffic flow.

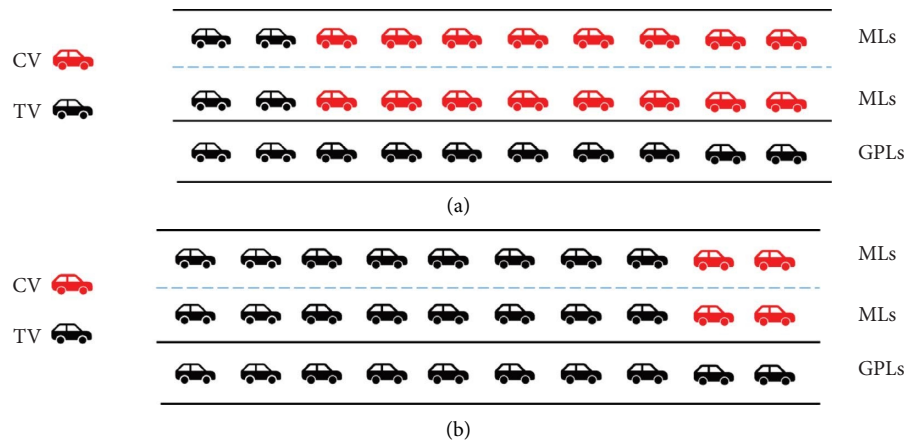

Figure 7: The arrangement of the mixed traffic flow on each lane in the case of penetration of 80% and 20%. (a) CV penetration rate of 80%. (b) CV penetration rate of 20%.

Table 5: The specific experiments.

Experiments	Measured indicators	Cases	CV lane-changing model	CV car-following model	CV penetration rate (%)
Experiment 1	Mixed traffic flow disturbance (amplitude, duration)	1	IDM (HC)	Aggressive-LC2013	80
		2	IDM (HC)	Normal-LC2013	80
		3	IDM (LC)	Aggressive-LC2013	80
		4	IDM (LC)	Normal-LC2013	80
		5	IDM (HC)	Aggressive-LC2013	20
		6	IDM (HC)	Normal-LC2013	20
		7	IDM (LC)	Aggressive-LC2013	20
		8	IDM (LC)	Normal-LC2013	20
Experiment 2	Mixed traffic flow safety (DRAC, TGAP)	1	IDM (HC)	Aggressive-LC2013	80
		2	IDM (HC)	Normal-LC2013	80
		3	IDM (LC)	Aggressive-LC2013	80
		4	IDM (LC)	Normal-LC2013	80
		5	IDM (HC)	Aggressive-LC2013	20
		6	IDM (HC)	Normal-LC2013	20
		7	IDM (LC)	Aggressive-LC2013	20
		8	IDM (LC)	Normal-LC2013	20
Experiment 3	Mixed traffic flow efficiency (flow, speed)	1	IDM (HC)	Aggressive-LC2013	80
		2	IDM (HC)	Normal-LC2013	80
		3	IDM (LC)	Aggressive-LC2013	80
		4	IDM (LC)	Normal-LC2013	80
		5	IDM (HC)	Aggressive-LC2013	20
		6	IDM (HC)	Normal-LC2013	20
		7	IDM (LC)	Aggressive-LC2013	20
		8	IDM (LC)	Normal-LC2013	20

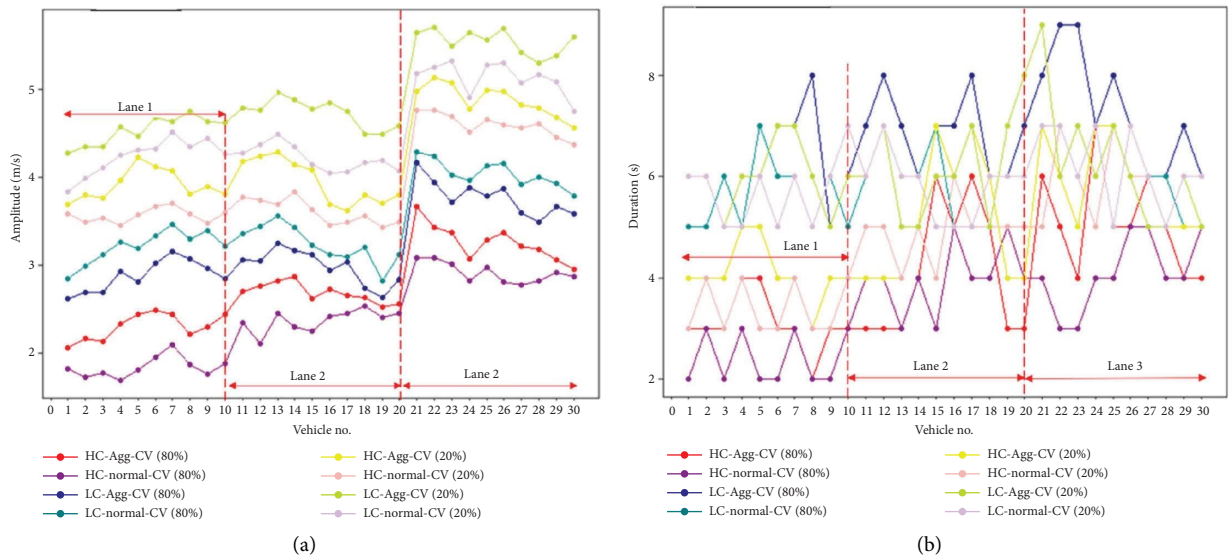

Figure 8: Comparison of traffic flow disturbance for every vehicle on three lanes based on arrangement 2. (a) Duration. (b) Amplitude.

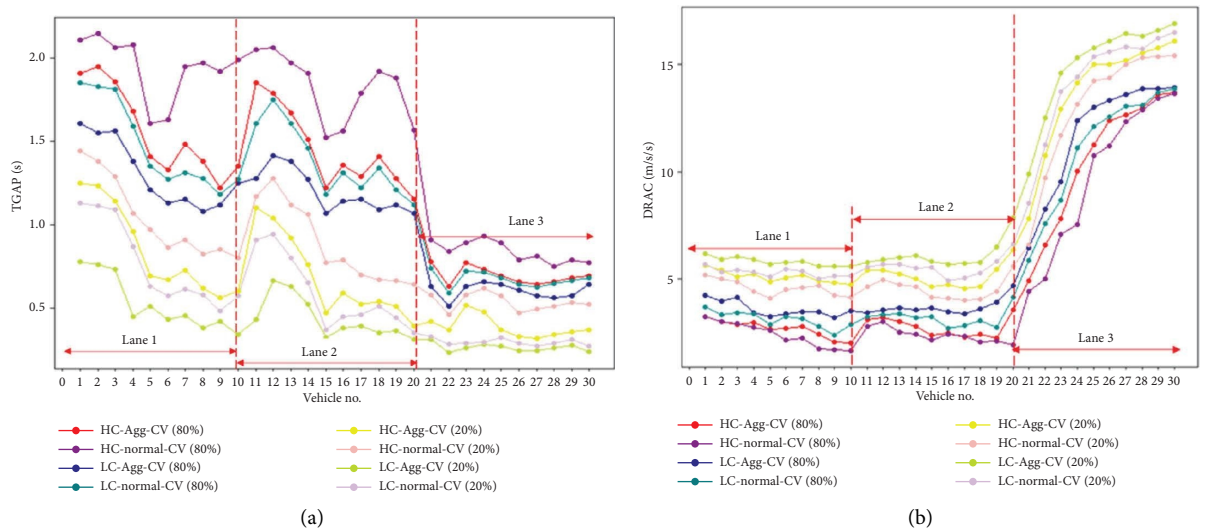

Figure 9: Comparison of traffic flow safety for every vehicle on three lanes based on arrangement 2. (a) TGAP. (b) DRAC.

and LC-aggressive-CV and HC-normal-CV and LC-normal-CV, respectively. And we can get the same conclusion in case of CV penetration rate being 20%.

Moreover, from lane 1 to lane 3, the gap between the eight cases gradually decreases. And compared with the mixed traffic flow with lower CV penetration rate, the mixed traffic flow with higher CV penetration rate corresponds to higher traffic flow safety.

4.5.3. Experiment 3 (Mixed Traffic Flow Efficiency). We set a detector every 10 meters in the traffic flow test section to measure the traffic flow efficiency at this location. The purpose of this experiment is to investigate the traffic flow efficiency of eight cases. Figure 10 displays that the traffic flow efficiency of higher CV penetration rate is higher than lower CV penetration rate. Meanwhile, there is a little difference in traffic flow efficiency corresponding to each case in uncongested section, but in congested section, this difference will be obvious. Compared to LC-CV, HC-CVs leads to higher traffic flow efficiency. And aggressive-CV leads to higher traffic flow efficiency than normal-CV.

4.6. Collaborative Evaluation Model. This study established the following collaborative evaluation model based on chosen indicators (traffic flow disturbance, safety, and efficiency) to quantify the overall efficiency in eight cases (shown in equation (25)). Average duration is not taken into consideration in the evaluation model due to the little

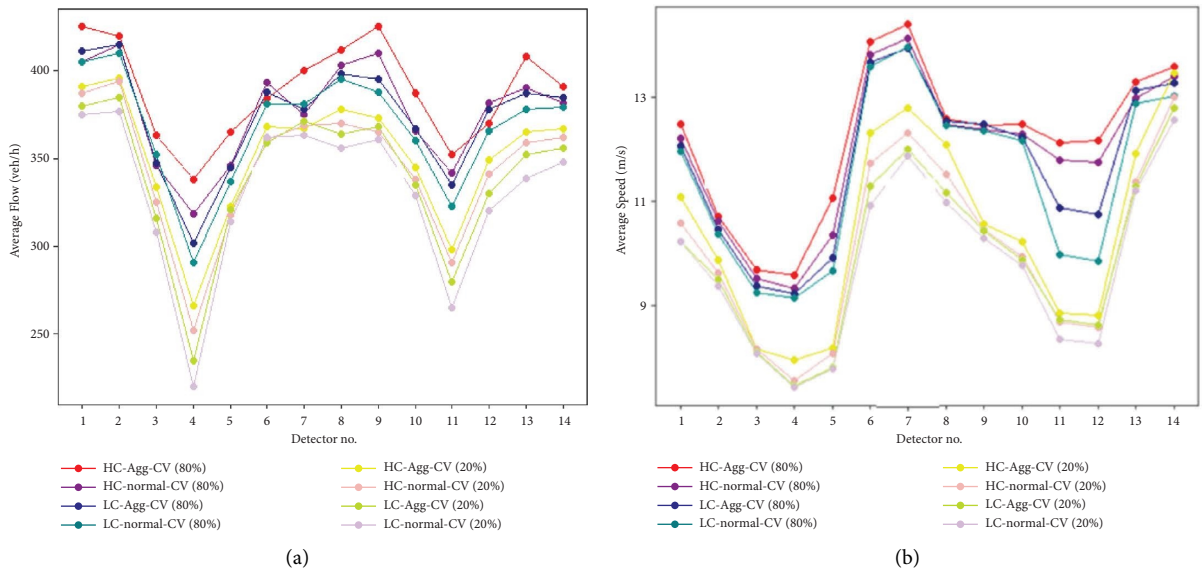

Figure 10: Comparison of average traffic flow efficiency for fourteen detector locations of overall traffic test section based on eight combinations of traffic flow arrangement and CV type. (a) Average flow. (b) Average speed.

Table 6: Basic parameters calculated in every composition.

Case	AverageFlow (veh/s)	AverageSpeed (m/s)	AverageAmplitude (m/s)	AverageTGAP (s)	AverageDRAC (m/s/s)
Case 1	0.12	12.18	3.178	0.83	5.86
Case 2	0.106	11.99	2.306	1.73	4.12
Case 3	0.104	11.7	3.97	0.63	7.07
Case 4	0.102	11.27	3.72	0.71	6.66
Case 5	0.098	10.44	3.55	0.64	6.55
Case 6	0.096	10.01	3.37	0.81	5.58
Case 7	0.094	9.94	4.47	0.41	8.52
Case 8	0.092	9.39	3.99	0.52	7.75

difference between eight cases in value of this indicator. The larger the K value, the greater the overall efficiency of this case.

$$K = \rho_1\left(\theta_1 \text{AverageFlow} + \theta_2 \text{AverageSpeed}\right) + \rho_2 \frac{1}{\text{AverageAmplitude}} + \rho_3 \frac{\text{AverageTGAP}}{\text{AverageDRAC}}, \tag{26}$$

where θ_1 and θ_2 represent the weights of flow and speed, respectively, and the values are set as 0.5 and 0.5 in this study; ρ_1, ρ_2, ρ_3 represent the weights of traffic flow efficiency, disturbance, and safety, which are set as different compositions of values in this study.

Table 6 displays the values of basic parameters in every composition. And we can further calculate the values of overall efficiency corresponding to eight cases (as shown in Figure 11).

We can conclude that in case of comprehensive consideration of traffic flow disturbance, efficiency, and safety, the overall efficiency value of mixed traffic flow with higher CV penetration rate is higher than that of mixed traffic flow with lower CV penetration rate. Moreover, CV drivers obeying CVs-IDM (HC) have higher value of overall efficiency than CV drivers obeying CVs-IDM (LC). In terms of aggressiveness, when CV penetration rate is 80%, CV drivers' behavior obeying normal-LC2013 leads to higher

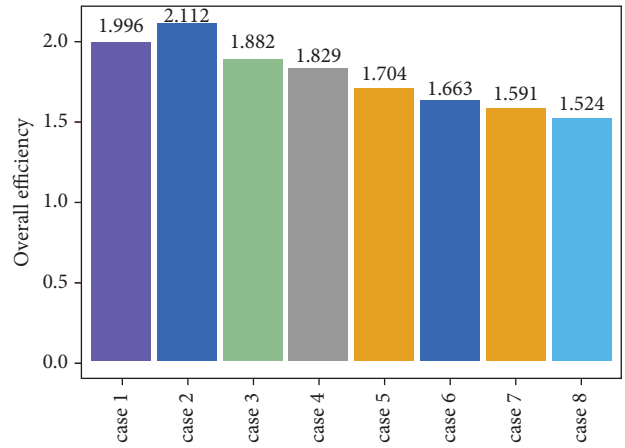

Figure 11: The overall efficiency of eight cases.

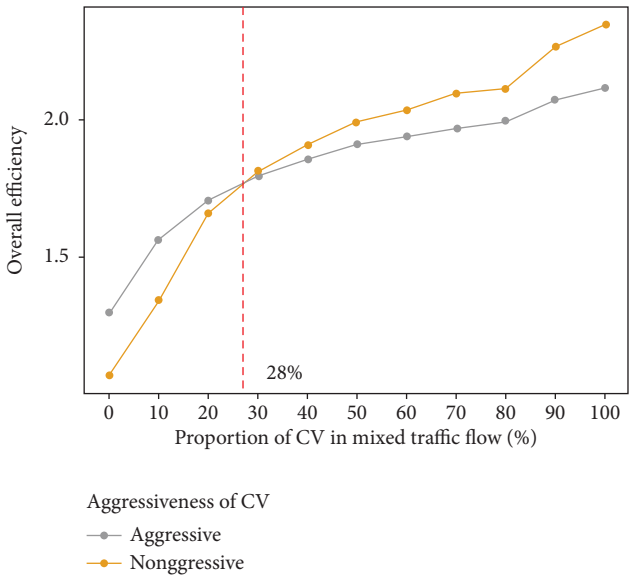

Figure 12: The comprehensive efficiency values of two degrees of CV drivers' aggressiveness in case of different CV proportions.

Table 7: The optimal CV type corresponding to different indicators.

Considered indicator	CV types
Mixed traffic flow disturbance	HC-normal-CV
Mixed traffic flow safety	HC-normal-CV
Mixed traffic flow efficiency	HC-aggressive-CV

overall efficiency. However, when CV penetration rate is 20%, CV drivers' behavior obeying aggressive-LC2013 leads to higher overall efficiency.

Furthermore, in order to study the penetration rate range suitable for normal-LC2013 and aggressive-LC2013, respectively, we reset the CV penetration rate in the previous experiment to 0%, 10%, 30%, 40%, 50%, 60%, 70%, 90%, and 100% and repeat the experiment (the results are shown in Figure 12).

Table 8: CV types corresponding to different CV penetration rates.

CV penetration rate (%)	CV type
0–28	HC-aggressive-CV
28–100	HC-normal-CV

5. Conclusion

The findings of this study have several important implications for policy and practice. Based on the trajectory data of CVs in the abovementioned study scene captured by UAV, we used the clustering method to divide the compliance of the CV driver to the information when performing car following and the aggressiveness when preforming lane changing into three clusters, respectively. Furthermore, we calibrated the parameters contained in three kinds of car-following models and three kinds of lane-changing models of the CV in the simulation experiments. The average error of parameter calibration in this paper is 12.5%, which is less than 13.3% mentioned in [4].

Secondly, we concluded that when the indicators (mixed traffic flow disturbance, safety, and efficiency) are considered separately, higher CV penetration leads to lower disturbance, higher safety, and higher efficiency based on above three experiments. Furthermore, we can summarize the CV types corresponding to lower disturbance, higher safety, and higher efficiency, respectively (as shown in Table 7) [34, 35].

Thirdly, considering the above three indicators comprehensively, we can conclude that when the CV penetration rate in the mixed traffic flow is lower than 28%, CV drivers obeying aggressive-LC2013 lead to higher overall efficiency; when the CV penetration rate in the mixed traffic flow is higher than 28%, CV drivers obeying normal-LC2013 lead to higher overall efficiency. Therefore, we can summarize specific measures to improve the overall efficiency of mixed traffic flow: increasing the CV penetration rate in the mixed traffic flow as much as possible. When the CV penetration rate is determined, set the CV type according to Table 8.

Data Availability

Data are included within the article.

Conflicts of Interest

The authors declare that they have no conflicts of interest.

Acknowledgments

This study was supported by the Yunnan Provincial Department of Education Science Research Fund Project (2023Y0769).

References

[1] M. Guériau, R. Billot, N. E. El Faouzi, J. Monteil, F. Armetta, and S. Hassas, "How to assess the benefits of connected vehicles? A simulation framework for the design of cooperative traffic management strategies," *Transportation Research Part C: Emerging Technologies*, vol. 67, pp. 266–279, 2016.

[2] S. Ilgin Guler, M. Menendez, and L. Meier, "Using connected vehicle technology to improve the efficiency of intersections," *Transportation Research Part C: Emerging Technologies*, vol. 46, pp. 121–131, 2014.

[3] J. E. Siegel, D. C. Erb, and S. E. Sarma, "A survey of the connected vehicle landscape—architectures, enabling technologies, applications, and development areas," *IEEE Transactions on Intelligent Transportation Systems*, vol. 19, no. 8, pp. 2391–2406, 2018.

[4] L. Zheng, T. Sayed, and M. Essa, "Validating the bivariate extreme value modeling approach for road safety estimation with different traffic conflict indicators," *Accident Analysis & Prevention*, vol. 123, pp. 314–323, 2019.

[5] Z. Zheng, S. Ahn, D. Chen, and J. Laval, "Applications of wavelet transform for analysis of freeway traffic: bottlenecks, transient traffic, and traffic oscillations," *Transportation Research Part B: Methodological*, vol. 45, no. 2, pp. 372–384, 2011.

[6] S. Yang, M. Du, and Q. Chen, "Impact of connected and autonomous vehicles on traffic efficiency and safety of an on-ramp," *Simulation Modelling Practice and Theory*, vol. 113, Article ID 102374, 2021.

[7] Z. Xu, Z. Jiang, G. Wang et al., "When the automated driving system fails: dynamics of public responses to automated vehicles," *Transportation Research Part C: Emerging Technologies*, vol. 129, Article ID 103271, 2021.

[8] C. Zhao, F. Liao, X. Li, and Y. Du, "Macroscopic modeling and dynamic control of on-street cruising-for-parking of autonomous vehicles in a multi-region urban road network," *Transportation Research Part C: Emerging Technologies*, vol. 128, Article ID 103176, 2021.

[9] H. Yu, R. Jiang, Z. He et al., "Automated vehicle-involved traffic flow studies: a survey of assumptions, models, speculations, and perspectives," *Transportation Research Part C: Emerging Technologies*, vol. 127, Article ID 103101, 2021.

[10] T. Li, F. Guo, R. Krishnan, A. Sivakumar, and J. Polak, "Right-of-way reallocation for mixed flow of autonomous vehicles and human driven vehicles," *Transportation Research Part C: Emerging Technologies*, vol. 115, no. C, Article ID 102630, 2020.

[11] H. Jiang, J. Hu, S. An, M. Wang, and B. B. Park, "Eco approaching at an isolated signalized intersection under partially connected and automated vehicles environment," *Transportation Research Part C: Emerging Technologies*, vol. 79, pp. 290–307, 2017.

[12] S. Gong and L. Du, "Cooperative platoon control for a mixed traffic flow including human drive vehicles and connected and autonomous vehicles," *Transportation Research Part B: Methodological*, vol. 116, pp. 25–61, 2018.

[13] M. S. Rahman, M. Abdel-Aty, J. Lee, and M. H. Rahman, "Safety benefits of arterials' crash risk under connected and automated vehicles," *Transportation Research Part C: Emerging Technologies*, vol. 100, pp. 354–371, 2019.

[14] A. Ghiasi, X. Li, and J. Ma, "A mixed traffic speed harmonization model with connected autonomous vehicles," *Transportation Research Part C: Emerging Technologies*, vol. 104, pp. 210–233, 2019.

[15] H. Liu, X. D. Kan, S. E. Shladover, X. Y. Lu, and R. E. Ferlis, "Modeling impacts of Cooperative Adaptive Cruise Control on mixed traffic flow in multi-lane freeway facilities," *Transportation Research Part C: Emerging Technologies*, vol. 95, pp. 261–279, 2018.

[16] P. Liu, Y. Du, L. Wang, and J. Da Young, "Ready to bully automated vehicles on public roads?" *Accident Analysis & Prevention*, vol. 137, no. C, Article ID 105457, 2020.

[17] J. I. Ge and G. Orosz, "Dynamics of connected vehicle systems with delayed acceleration feedback," *Transportation Research Part C: Emerging Technologies*, vol. 46, pp. 46–64, 2014.

[18] M. H. Rahman, M. Abdel-Aty, and Y. Wu, "A multi-vehicle communication system to assess the safety and mobility of connected and automated vehicles," *Transportation Research Part C: Emerging Technologies*, vol. 124, Article ID 102887, 2021.

[19] A. Olia, H. Abdelgawad, B. Abdulhai, and S. N. Razavi, "Assessing the potential impacts of connected vehicles: mobility, environmental, and safety perspectives," *Journal of Intelligent Transportation Systems*, vol. 20, no. 3, pp. 229–243, 2016.

[20] D. Chen, A. Srivastava, S. Ahn, and T. Li, "Traffic dynamics under speed disturbance in mixed traffic with automated and non-automated vehicles," *Transportation Research Part C: Emerging Technologies*, vol. 113, pp. 293–313, 2020.

[21] B. Van Arem, C. J. G. Van Driel, and R. Visser, "The impact of cooperative adaptive cruise control on traffic-flow characteristics," *IEEE Transactions on Intelligent Transportation Systems*, vol. 7, no. 4, pp. 429–436, 2006.

[22] P. Wagner, "Traffic control and traffic management in a transportation system with autonomous vehicles," *Autonomous Driving: Technical, Legal and Social Aspects*, pp. 301–316, 2016.

[23] H. Shi, Y. Zhou, K. Wu, X. Wang, Y. Lin, and B. Ran, "Connected automated vehicle cooperative control with a deep reinforcement learning approach in a mixed traffic environment," *Transportation Research Part C: Emerging Technologies*, vol. 133, Article ID 103421, 2021.

[24] E. Amini, A. Omidvar, and L. Elefteriadou, "Optimizing operations at freeway weaves with connected and automated vehicles," *Transportation Research Part C: Emerging Technologies*, vol. 126, Article ID 103072, 2021.

[25] D. Jia, D. Ngoduy, and H. L. Vu, "A multiclass microscopic model for heterogeneous platoon with vehicle-to-vehicle communication," *Transportation Business: Transport Dynamics*, vol. 7, no. 1, pp. 311–335, 2018.

[26] S. Learn, J. Ma, K. Raboy, F. Zhou, and Y. Guo, "Freeway speed harmonisation experiment using connected and automated vehicles," *IET Intelligent Transport Systems*, vol. 12, no. 5, pp. 319–326, 2018.

[27] A. Sharma, Y. Ali, M. Saifuzzaman, Z. Zheng, and M. M. Haque, "Human factors in modelling mixed traffic of traditional, connected, and automated vehicles[C]//Advances in Human Factors in Simulation and Modeling," in *Proceedings of the AHFE 2017 International Conference on Human Factors in Simulation and Modeling*, pp. 262–273, New York, NY, USA, July 2017.

[28] P. Songchitruksa, A. Bibeka, L. I. Lin, and Y. Zhang, "Incorporating driver behaviors into connected and automated vehicle simulation[R]," *Center for Advancing Transportation Leadership and Safety (ATLAS Center)*, 2016.

[29] T. Kim, *Assessment of Vehicle-To-Vehicle Communication-Based Applications in an Urban network[D]*, Virginia Polytechnic Institute and State University, Virginia, USA, 2015.

[30] Q. Li and T. Z. Qiu, "Study on CACC algorithm for platoons at signalized intersections to improve traffic flow efficiency," in *Proceedings of the COTA International Conference of Transportation Professionals[M]//CICTP 2020*, pp. 5322–5334, Xi'an, China, August 2020.

[31] B. Friedrich, "The effect of autonomous vehicles on traffic," *Autonomous Driving: Technical, legal and social aspects*, pp. 317–334, 2016.

[32] D. Ni, J. Li, S. Andrews, and H. Wang, "A methodology to estimate capacity impact due to connected vehicle technology," *International Journal of Vehicular Technology*, vol. 2012, pp. 1–10, 2012.

[33] A. Sharma, Z. Zheng, J. Kim, A. Bhaskar, and M. Mazharul Haque, "Assessing traffic disturbance, efficiency, and safety of the mixed traffic flow of connected vehicles and traditional vehicles by considering human factors," *Transportation Research Part C: Emerging Technologies*, vol. 124, Article ID 102934, 2021.

[34] J. Jang, J. Ko, J. Park, C. Oh, and S. Kim, "Identification of safety benefits by inter-vehicle crash risk analysis using connected vehicle systems data on Korean freeways," *Accident Analysis & Prevention*, vol. 144, Article ID 105675, 2020.

[35] M. Saffarian, J. C. F. De Winter, and R. Happee, "Automated driving: human-factors issues and design solutions," *Proceedings of the Human Factors and Ergonomics Society Annual Meeting*, Sage Publications, vol. 56, no. 1, pp 2296–2300, Sage CA: Los Angeles, CA, 2012.